Variable Stars in the Magellanic Clouds: Results from OGLE and SIRIUS

Yoshifusa Ita[1]⋆, Toshihiko Tanabé[1], Noriyuki Matsunaga[1], Yasushi Nakajima[2], Chie Nagashima[2], Takahiro Nagayama[2], Daisuke Kato[2], Mikio Kurita[2], Tetsuya Nagata[2], Shuji Sato[2], Motohide Tamura[3], Hidehiko Nakaya[4] and Yoshikazu Nakada[1,5]

[1]*Institute of Astronomy, School of Science, The University of Tokyo, Mitaka, Tokyo 181-0015, Japan*

[2]*Department of Astrophysics, Nagoya University, Chikusa-ku, Nagoya 464-8602, Japan*

[3]*National Astronomical Observatory of Japan, Mitaka, Tokyo 181-8588, Japan*

[4]*Subaru Telescope, National Astronomical Observatory of Japan, 650 North A'ohoku Place, Hilo, HI 96720, U.S.A.*

[5]*Kiso Observatory, School of Science, The University of Tokyo, Mitake, Kiso, Nagano 397-0101, Japan*

ABSTRACT

We have performed a cross-identification between OGLE-II data and single-epoch SIRIUS near-infrared (NIR) JHK survey data in the Large and Small Magellanic Clouds (LMC and SMC, respectively). After eliminating obvious spurious variables, variables with too few good data and variables that seems to have periods longer than the available baseline of the OGLE-II data, we determined the pulsation periods for 9,681 and 2,927 variables in the LMC and SMC, respectively.

Based on these homogeneous data, we studied the pulsation properties and metallicity effects on period-K magnitude (PK) relations by comparing the variable stars in the Large and Small Magellanic Clouds. The sample analyzed here is much larger than the previous studies, and we found the following new features in the PK diagram: (1) variable red giants in the SMC form parallel sequences on the PK plane, just like those found by Wood (2000) in the LMC; (2) both of the sequences A and B of Wood (2000) have discontinuities, and they occur at the K-band luminosity of the TRGB; (3) the sequence B of Wood (2000) separates into three independent sequences $B^{\pm}$ and C'; (4) comparison between the theoretical pulsation models (Wood & Sebo 1996) and observational data suggests that the variable red giants on sequences C and newly discovered C' are pulsating in the fundamental and first overtone mode, respectively; (5) the theory can not explain the pulsation mode of sequences $A^{\pm}$ and $B^{\pm}$, and they are unlikely to be the sequences for the first and second overtone pulsators, as was previously suggested; (6) the zero points of PK relations of Cepheids in the metal deficient SMC are fainter than those of LMC ones by ≈ 0.1 mag but those of SMC Miras are brighter than those of LMC ones by ≈ 0.13 mag (adopting the distance modulus offset between the LMC and SMC to be 0.49 mag and assuming the slopes of the PK relations are the same in the two galaxies), which are probably due to metallicity effects.

Key words: galaxies: Magellanic Clouds – stellar content – stars: AGB and post-AGB – variables – infrared: stars – surveys

1 INTRODUCTION

The Large and Small Magellanic Clouds offer us the opportunity to study the stellar evolution. They are close enough to resolve each stellar populations with relatively small telescopes and yet far enough to neglect their depth, so that we can reasonably consider that all stars in them are at the same distance from us.

Many observations have been carried out toward the LMC and SMC, especially for the variable stars to study the relationship between the pulsation period and the luminosity (*PL* relationship). There is a long standing question related to the *PL* relationship, whether it depends on metallicity or not. A controversy still exists between observations and theories (e.g., Alibert et al. 1999 and references therein for Cepheid variables; Wood & Sebo 1996, Glass et al. 1995, Feast, Whitelock & Menzies 2002 for long-period variables). Because the *PL* relationship is of fundamental importance for the determination of the extragalactic distance

⋆ E-mail: yita@ioa.s.u-tokyo.ac.jp

scale, a homogeneous survey of variable stars in different environments is needed.

Thanks to the gravitational microlensing search projects (OGLE, e.g., Udalski, Kubiak & Szymański 1997; MACHO, e.g., Alcock et al. 2000; EROS, e.g., Afonso et al. 1999; MOA, e.g., Bond et al. 2001), a large number of variable stars have been found in the Magellanic Clouds. Wood et al. (1999) analyzed the data from MACHO survey in the 0.25 square degree area of the LMC bar and showed that the variable red giants form parallel sequences in the period-magnitude plane. Cioni et al. (2001) and Lebzelter, Schultheis & Melchior (2002) confirmed the results of Wood (2000) using data from EROS microlensing survey and AGAPEROS variable star catalog (Melchior, Hughes & Guibert 2000), respectively, both in the 0.25 square degree area of the LMC bar.

In this paper, we study the OGLE variables in the 3 square degrees along the LMC bar (see figure 1 of Ita et al. 2002) and in the 1 square degree area of the central part of the SMC (figure 1). The OGLE variables have been cross-identified with the SIRIUS NIR survey data and their pulsation periods were determined by applying the Phase Dispersion Minimization technique to the OGLE data. We classify the variable stars on the *PK* plane, and discuss the properties of each group. The environmental effect on *PK* relations is discussed by comparing variable stars in the Large and Small Magellanic Clouds.

2   DATA

2.1   IRSF/SIRIUS

We are now conducting a NIR *JHK* monitoring survey toward the Magellanic Clouds using the InfraRed Survey Facility (IRSF) at Sutherland, South African Astronomical Observatory. The IRSF consists of a specially constructed 1.4m alt-azimuth telescope to which is attached a large-format 3-channel infrared camera, SIRIUS (Simultaneous three-colour InfraRed Imager for Unbiased Surveys). The SIRIUS can observe the sky in *J H* and K_s bands simultaneously and has a field of view of about 7.7 arcmin square with a scale of 0.45 arcsec/pixel. Details of the instrument are found in Nagashima et al. (1999) and Nagayama et al. (2002).

We have been monitoring a total area of 3 square degrees along the LMC bar since December 2000, and a total area of 1 square degree around the SMC center since July 2001. Figure 1 shows the monitoring area in the SMC. Details and some first results of the LMC survey are found in Ita et al. (2002) (hereafter referred to as Paper I). In the present paper we deal with the single-epoch data from the monitoring survey.

2.1.1   Photometry

All data were reduced in the same way using the SIRIUS pipeline (Nakajima, private communication) and a single image comprises 100 dithered 5 sec exposures. Photometry was performed on the dithered images with DoPHOT in the fixed position mode (Schechter, Mateo & Saha 1993). The magnitudes are referred to the Las Campanas Ovservatory (LCO) system ones based on observations of a few dozen stars from Persson et al. (1998). In the system conversion, colour terms have been considered by observing red stars in table 3 of Persson et al. The photometry has a signal-to-noise ratio (S/N) of about 20 at 16.9, 16.8 and 16.0 mag in *J*, *H* and
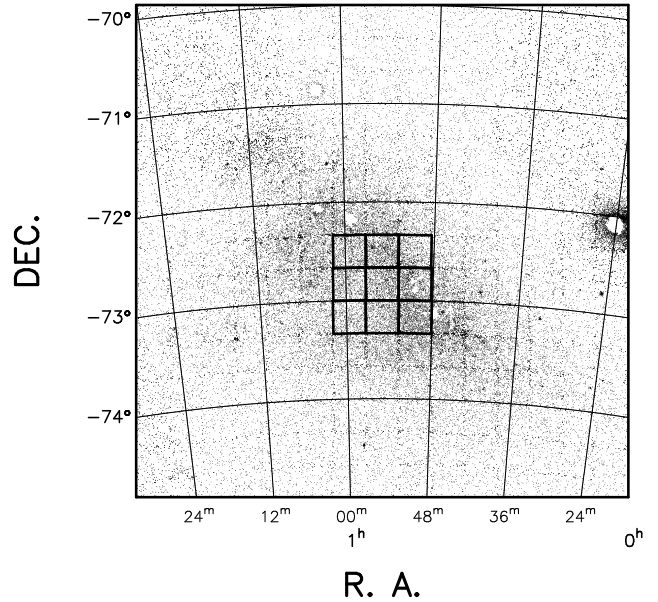

Figure 1. A schematic map of the monitoring region in the SMC. Each mesh has a side of 20 arcmin and consists of 9 sub-meshes, which correspond to the field of view of the SIRIUS. The background stars are drawn from the GSC2.2 catalog. Stars brighter than 16th magnitude at F_{gsc} located in the total area of 25 square degree centered on $(\alpha_{2000}, \delta_{2000}) = (0^h 55^m 00.0^s, -70° 30′ 00.0″)$ are plotted.

K, respectively. Typical photometric errors are tabulated in table 1 of Paper I.

2.1.2   Source selection

LMC:
In the three square degree survey area, 1,593,248 sources were detected by DoPHOT. Because of the scan overlaps, there should be many multiple entries of a single source in the original sample. We eliminated such multiple entries based on (1) spatial proximity ($|\Delta r| \leqslant 0.5″$) and (2) difference in photometry ($|\Delta m_{J,HandK}| \leqslant 0.1$ mag). It leaves 1,305,983 sources. Further, requiring detections at least two of the three wave bands leaves 789,929 sources.

In Paper I, we used the allowed discrepancy $|\Delta r|$ of 1.5″, instead of the present value of 0.5″. This was because the celestial coordinates were calculated by referencing the USNO catalog instead of the Guide Star Catalog II (GSC2.2, see section 2.1.3.). We can find substantial number of positional reference stars by using the GSC2.2 catalog, and this greatly improved the accuracy of the positioning.

SMC:
In the one square degree survey area, 257,637 sources were detected by DoPHOT. Multiple entries were eliminated in the same manner as we did in the LMC. It leaves 210,566 sources. Further, requiring detections at least two of the three wave bands leaves 107,376 sources.

2.1.3   SIRIUS data

In table 1 we summarize the number of sources detected in each wave band. Hereafter, we refer these 789,929 and 107,376 sources as the SIRIUS data. Although many stars were detected only in two wave bands, these stars hardly affect the results of this paper.

Table 1. Breakdown list of the SIRIUS data

Wavebands				Number	
				LMC	SMC
J	+	H	+	K	596,913	85,491
J	+	H			75,812	15,173
		H	+	K	114,827	6,693
J	+			K	2,377	19
Total				789,929	107,376

Also, although SIRIUS *JHK* photometries are single-epoch ones, it should not affect the results so much, because the pulsation amplitudes of variable stars are usually small in the infrared (except for Mira variables, but still the results should be statistically fair because of large number of available data).

The SIRIUS data were corrected for the interstellar absorption based on the relations in Koornneef (1982), assuming $R = 3.2$. We adopted $(A_J, A_H, A_K) = (0.129, 0.084, 0.040)$ and $(0.082, 0.053, 0.025)$, corresponding to the total mean reddenings of $E_{B-V} = 0.137$ and 0.087 as derived by Udalski et al. (1999a) for the OGLE's observing fields in the LMC and SMC, respectively.

2.1.4 Astrometry

Celestial coordinates of the sources detected by the SIRIUS were systematically calculated in the International Celestial Reference System (ICRS) by referencing the Guide Star Catalog II (STScI 2001). The astrometric precision of the SIRIUS data is expected to be the same as that of GSC 2.2 catalog, i.e., better than $0.5''$ in most cases (Tanabé et al. in preparation).

2.2 OGLE

Thanks to the microlensing surveys (OGLE, MACHO, EROS, MOA), a large number of variable stars were found as the natural by-products. In particular, the Optical Gravitational Lensing Experiment (OGLE) project has been monitoring the central parts of the Magellanic Clouds in the *BVI* wave bands and the *I* band time-series data (OGLE-II; Udalski et al. 1997) is now available over the Internet (OGLE homepage; http://sirius.astrouw.edu.pl/~ogle/).

2.2.1 Cross-identification of the SIRIUS sources and the OGLE variables

The SIRIUS data and all the stars found by the OGLE survey in the Magellanic Clouds have been cross-identified using a simple positional correlation. In the very strict sense, the OGLE survey does not fully cover the SIRIUS survey area, and some very small areas are not included in the OGLE. However, it never affect any conclusions in this paper.

LMC:
There are 49,008 OGLE variables in the OGLE/SIRIUS overlapped 3 square degree area in the LMC. The identification was made in two steps. First a search radius of $3''$ was used, finding 35,726 matches. Plotting the offsets between the SIRIUS coordinates and the OGLE coordinates revealed that there are small median astrometric shifts between them; the median differences are $-0.80''$ in right ascension (R.A.) and $0.10''$ in declination (DEC). Second, the OGLE coordinates were corrected for these offsets, and a search radius of $3''$ was used again. We finally found 35,783 matches with an
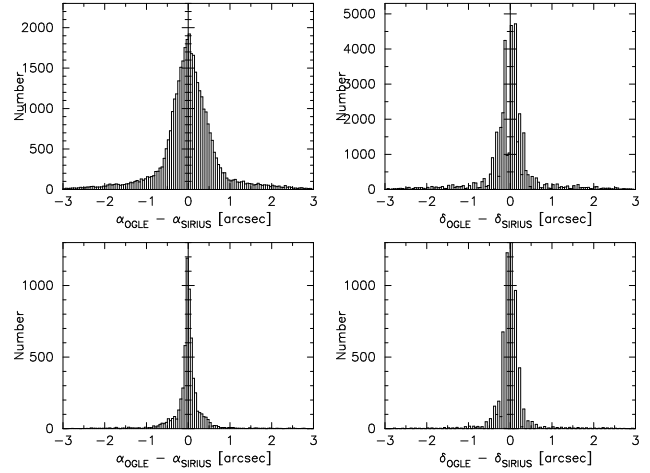

Figure 2. Histogram of the positional difference between the SIRIUS coordinates and the OGLE coordinates in $0.05''$ bins for the cross-identified stars in the LMC (upper panel) and the SMC (lower panel).

rms error in the difference between SIRIUS and OGLE coordinates $0.68''$ in R.A. and $0.63''$ in DEC, respectively.

SMC:
There are 7,345 OGLE variables in the OGLE/SIRIUS overlapped 1 square degree area in the SMC. The identification was made in the same way as we did in the LMC. First a search radius of $3''$ was used, finding 6,118 matches. The offsets between the SIRIUS coordinates and the OGLE coordinates are $0.02''$ in R.A. and $-0.40''$ in DEC. After correcting the OGLE coordinates for these median offsets, a search radius of $3''$ was used again. We finally found 6,103 matches with an rms error in the difference between SIRIUS and OGLE coordinates $0.41''$ in R.A. and $0.38''$ in DEC, respectively.

We show the histogram of positional differences of the finally identified stars in Figure 2. It is clear that the positional differences are smaller than $1''$ for most of the identified stars (29,228 out of 35,783 stars or 81.7% in the LMC, and 5,745 out of 6,103 stars or 94.1% in the SMC).

2.2.2 Period determination

We applied the Phase Dispersion Minimization (PDM) technique to the OGLE data to determine the light variation periods of the cross-identified stars. This technique is described in detail by Stellingwerf (1978) and here we show only the outline of the technique we used.

We represent the observational dataset as (x_i, t_i), where x is the magnitude, t is the observation time and i denotes the ith observation. We assume that there are N observations in all ($i = 1, N$). Let V be the variance of the magnitude of the original dataset, given by

$$V = \sum_{i=1}^{N} (x_i - \bar{x})^2 / (N - 1), \qquad (1)$$

where $\bar{x}$ is the mean; $\sum x_i / N$. First, the x_i and t_i are folded with a trial period and the full phase space $[0, 1)$ is divided into an appropriate (user-specified) number of bins (there are N_B bins in all, i.e., $j = 1, N_B$). Second, the variance v_j of magnitude of each bin and the mean variance $\bar{v}$ of them are calculated, namely,

$$\bar{v} = \sum_{j=1}^{N_B} v_j / N_B. \qquad (2)$$

Table 2. Used resolution in period search

trial period [day]		
start($\geqslant$)	end($<$)	resolution [day]
0.1	1.0	0.00001
1.0	5.0	0.0001
5.0	10.0	0.001
10.0	100.0	0.01
100.0	1000.0	0.1

Third, the statistic parameter θ, which is defined as

$$\theta = \bar{v}/V, \qquad (3)$$

is calculated for the trial period. These three processes are then repeated for the next trial period (i.e., $P_{\text{trial, new}} = P_{\text{trial, old}} +$ resolution; see below). The θ is a measure of the regularity of the light variation or the scatter about the mean light curve, being hopefully near 0 for the very regular light variation with true period and near 1 for the irregular light variation without any distinctive periodicity or for the incorrect period. Hereafter, we call stars with small θ ($\leqslant 0.55$) as "regularly pulsating variables", and the others (> 0.55) as "less regularly pulsating variables".

We searched the minimum of the θ throughout the trial periods that start from 0.1 and end in 1,000 days. The trial periods were incremented by variable step values (= resolution), which are summarized in table 2. For all of the 35,783 (LMC) and 6,103 (SMC) matched stars, their original light curve, θ spectra and the folded light curve are carefully eye-inspected, and the obvious spurious data points were eliminated. We assigned one pulsation period to each variable star, and the multi-periodic stars (e.g., Bedding et al. 1998) were not analyzed in this paper. It should be noted that the total available baseline of the OGLE-II data is about 1,200 days and we did not try to determine the light variation period for the variables that seem to have the period longer than 1,000 days. Also, we did not try to determine the period for the variables that have too few good data points and that seem to hardly show any periodicity. The OGLE-II survey data has yearly blank phases that could be a problem for variable stars with pulsation period of about a year. However, experimentations showed that these yearly gaps hardly affect the period determination, and it is the virtue of the PDM technique. In very rare cases, the yearly gaps may unfortunately coincide with the timing of the peak luminosities. They can affect the determination of pulsation amplitude, but still, such cases should be very rare. Finally, we determined the light variation periods for 9,681 and 2,927 OGLE variables in the LMC and SMC, respectively.

3   DISCUSSION

3.1   *K* magnitude distribution

Many low-amplitude variables were newly discovered by the aforementioned optical surveys. The vast majority are at the luminosities below the TRGB. Alves et al. (1998) suggested that they are AGB stars in the early evolutionary phase prior to entering the thermal-pulsing phase of the AGB. In Paper I, we found that the *K* magnitude distribution of the variable red giants in the LMC has two peaks; one is well above the TRGB, consisting genuine AGB variables and the other is just around the TRGB.

In figure 3, we show the *K* magnitude distribution $N(K)$ ($dK = 0.05$ mag) of the SIRIUS data. The discontinuity in the $N(K)$ is clearly seen around $K \approx 12.1$ (upper panel) and ≈ 12.7 (lower
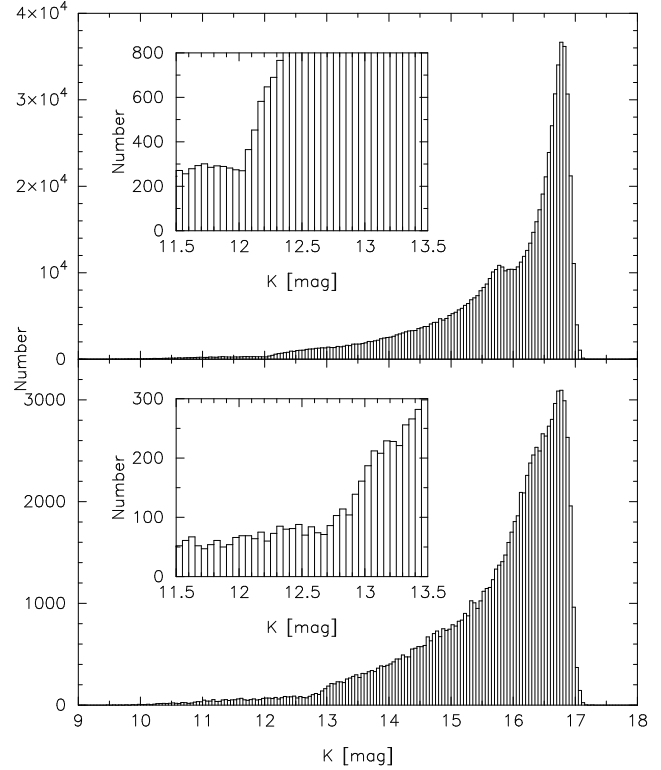

Figure 3. The *K* magnitude distribution differentiated by 0.05 mag bins of the SIRIUS data in the LMC (upper panel) and the SMC (lower panel). Closeup around the TRGB is shown in the inset.

panel), which corresponds to the TRGB of the LMC and SMC, respectively. Figure 4 is the same diagram as the figure 3, but the 9,681 and 2,927 OGLE/SIRIUS variables in the LMC and SMC are shown. It is clear that there is a "pile-up" around the *K*-band luminosity of the TRGB in both two galaxies. In Paper I, we concluded that a significant fraction of the constituent variable stars of the second peak could be on the RGB. Of course there may be faint AGB variables, but there is no reason to assume, according to models, that they accumulate at the TRGB.

3.2   Period-*K* magnitude diagram

Wood (2000) found that radially pulsating red giants in the LMC form "three" distinctive parallel sequences in the *PK* plane. He characterized the complex variability of the red giants by the pulsation modes, which are an important probe of the internal structure of the stars. Wood et al. (1999) suggested that Mira variables are fundamental mode pulsators, while so-called semi-regular variables can be pulsating in the first, second or even higher overtone mode, by comparison of observations with theoretical models. However, a controversy still exists on the pulsation mode of Mira variables. Diameter measurements of Mira variables in the Milky Way indicates first overtone pulsation (e.g., Haniff, Scholz & Tuthill 1995, Whitelock & Feast 2000), while observations of radial velocity variation favor fundamental mode pulsation for Mira variables (e.g., Bessell, Scholz & Wood 1996).

We show the relationship between the determined pulsation periods and the *K* magnitudes of the cross-identified variables in figure 5. We found that the variable red giants in the SMC form parallel sequences on the *PK* plane, just like those found by Wood
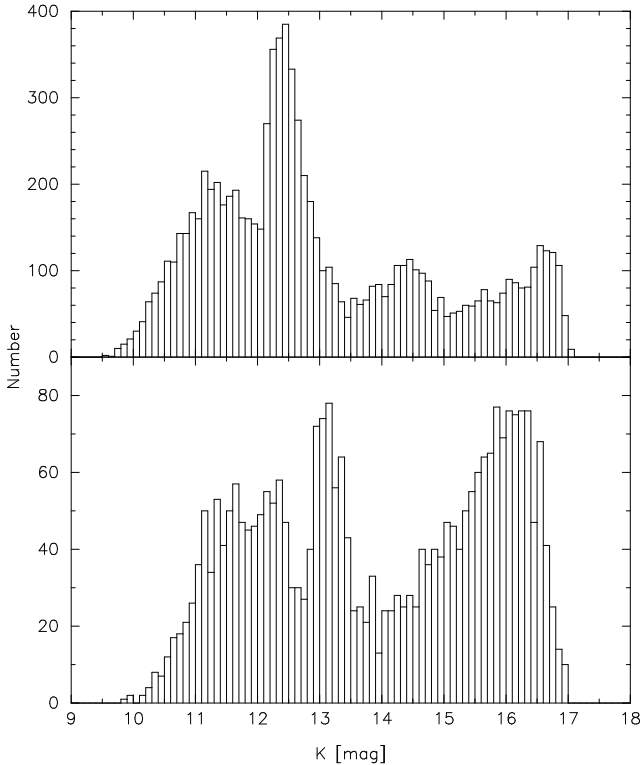
Figure 4. The *K* magnitude distribution differentiated by 0.1 mag bins of the OGLE/SIRIUS 9,681 and 2,927 variables in the LMC (upper panel) and the SMC (lower panel), respectively.

Figure 5. Period-*K* magnitude diagram for OGLE variables in the LMC (upper panel) and the SMC (lower panel).

(2000) in the LMC. In the LMC *PK* diagram, bunch of variable stars exist in the faint magnitude ($K \lesssim 15.0$) and very short period ($\log P \lesssim -0.1$) region. Considering their location on the *PK* plane, they are likely to be RR Lyrae variables. Compared to the LMC *PK* diagram, the SMC one is a bit scattered. This is probably due to the difference in the intrinsic depth of the two galaxies, because the LMC has a nearly face on orientation (Westerlund 1997), and Groenewegen (2000) obtained the total front-to-back depths of 0.043 mag for the LMC and 0.11 mag for the SMC, respectively.

In figure 6, we again show the *PK* relationship of variable stars in the Magellanic Clouds. In this diagram, we divided variable stars into four types according to their $J - K$ colours and θ as is shown on the upper-left corner of the figure. The labels of the sequences are named in analogy to the ones found in the LMC by Wood (2000) (except C', *F* and *G*). While Cioni et al. (2001) found no objects on sequence *A* from their EROS/DENIS variables in the LMC, this sequence is clearly seen in both galaxies. This is essentially the same diagram as the one obtained by Wood (2000). However, the sample used here is much larger than those of previous studies, and we can see new features in the figure: (1) the sequences *A* and *B* of Wood (2000) are found to be composed of the upper and lower sequences A^+, B^+, and A^-, B^-; (2) the sequence *B* of Wood (2000) separates into three independent sequences $B^\pm$ and C'; (3) radially pulsating red giants form actually "four" parallel sequences (A, B, C' and *C*).

3.2.1 *Less regularly pulsating variables*

Most of the less regularly pulsating variables reside in the sequences *A* and *B*, and show small pulsation amplitudes ($\Delta I \lesssim 0.2$ mag, but some of the *B* stars have ΔI of about 0.4 mag). Al-
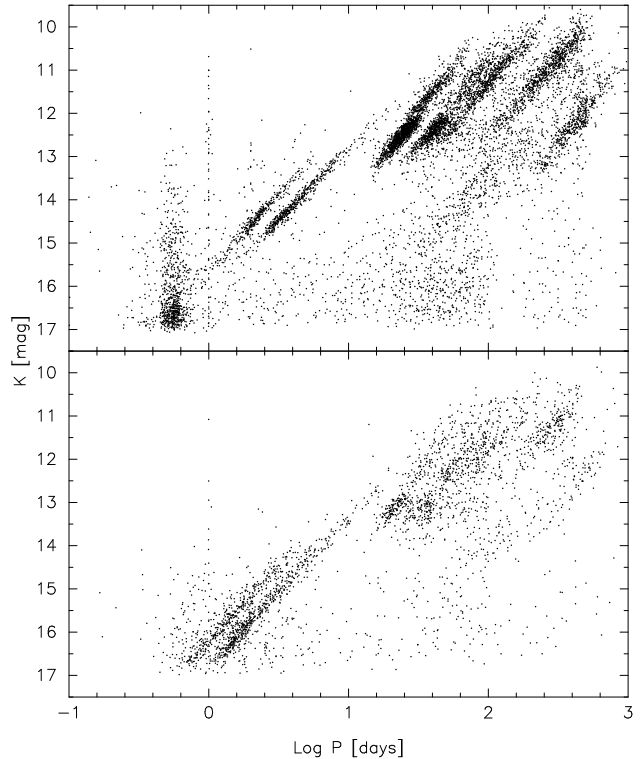
though it is not mentioned in Wood (2000), his sequences *A* and *B* are densely populated at fainter magnitudes, and a discernible gap around the TRGB can be seen in his diagram (see his figure 1). This gap also presents in our diagram around the *K*-band luminosity of the TRGB ($K \sim 12.1$ in the LMC and ~ 12.7 in the SMC), which we roughly estimated in section 3.1. Also, in the LMC, a horizontal misalignment of the sequences apparently occurs at the TRGB. One possible explanation for the discontinuity is that neither sequences *A* nor *B* are single sequences, but each of them is composed of two independent sequences. So we subdivided the sequences *A* and *B* into A^+, B^+ and A^-, B^-, where the + and − correspond to the luminosity, being brighter than $K = 12.1$ (LMC) or 12.7 (SMC) and fainter than it, respectively.

Since the sequences A^+ and B^+ exceed the *K*-band luminosity of the TRGB, they consist of intermediate-age population and/or metal-rich old population AGB stars. However, the interpretation of the sequences A^- and B^- is difficult. If the metal-poor and old AGB stars pulsate in the same mode as the more massive stars on the sequences A^+ or B^+, they should be located on the sequences A^- or B^- because they do not exceed the TRGB luminosity. The question is whether the sequences A^- and B^- contain RGB pulsators or not. If AGB stars alone make up the A^- and B^- as well as A^+ and B^+ sequences, the small gap and the horizontal shift between them needs to be explained. If A^- and B^- stars, at least some of them, are pulsating on the RGB, then the discontinuity between the − and + sequences is understood in terms of different evolutionary stages. If we could apply the same period-temperature relation as that for Mira variables (Alvarez & Mennessier 1997) to the A^- and A^+ stars, the period shift of $\delta \log P = -0.083$ between the two sequences at the TRGB ($K = 12.1$, see table 3) corresponds to the temperature difference of $\delta \log T_{\rm eff} \approx 0.015$. This
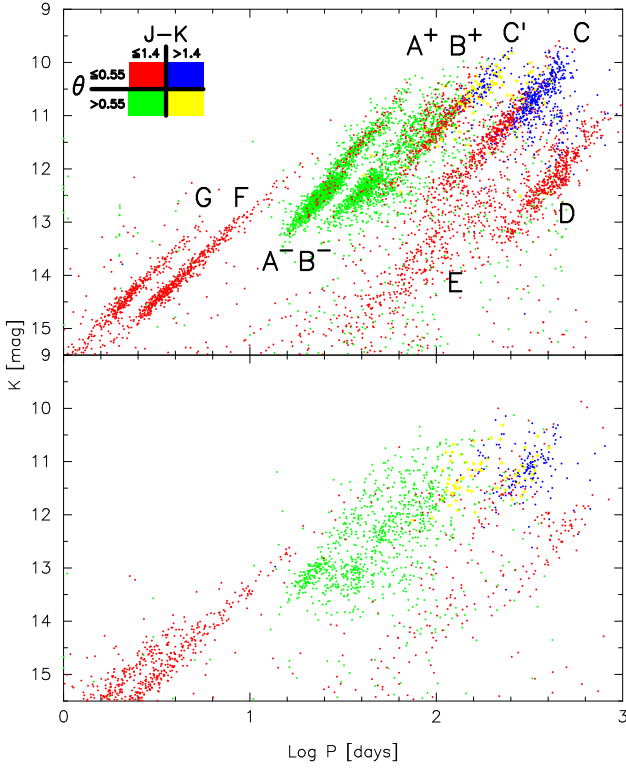
Figure 6. Period-*K* magnitude diagram for OGLE variables in the LMC (upper panel) and the SMC (lower panel). Variable stars are classified into four types according to their $J - K$ colours and θ. The labels of the sequences are named in analogous to the sequences found by Wood (2000) in the LMC (except C', F and G, see text).

is in good agreement with the temperature difference between the AGB and RGB stars with the TRGB luminosity, predicted by the stellar evolutionary model for stars with 1∼2 M$_\odot$ in the LMC (Castellani et al. 2003). Though we prefer the RGB interpretation, it should be noted that a definitive answer has not been obtained.

3.2.2   Regularly pulsating variables

Figure 7 shows the comparison between the observational period-*K* magnitude sequences of pulsating red giants in the LMC and the theoretical models calculated by Wood & Sebo (1996). The location of sequence *C* is consistent with the LMC Mira sequence (Feast et al. 1989). After classifying stars by their regularity of light variation, we discovered a new sequence C'. Most of the stars on sequence C' are regularly pulsating just like those on *C*, but their amplitudes are smaller than those of the *C* stars. We note, however, that the amplitudes of stars on sequence C' are larger than those of stars on *B*. The observed periods, luminosities and period ratio of sequences *C* and C' agree very well with those of the theoretical fundamental (P_0) and first overtone mode (P_1) pulsation models (Wood & Sebo 1996). Also, the theory predicts that overtone pulsators have smaller amplitudes than fundamental ones. Therefore, all of the above observational facts and the agreements with the theory could be naturally explained if we consider that the stars of sequences *C* and C' are Mira variables pulsating in the fundamental and first overtone mode, respectively. However, the pulsation theory cannot reproduce the period ratio of the observed sequences *A* and *B*. To explain their pulsation modes, a new theoretical model is needed.
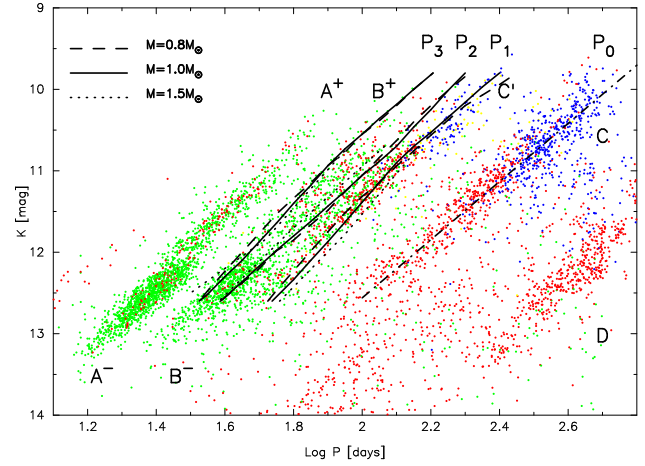

Figure 7. Period-*K* magnitude relations of variable red giants compared with theoretical model of Wood & Sebo (1996). Their models for stars of masses of 0.8, 1.0 and 1.5 M$_\odot$ pulsating in the fundamental (P_0, they forced theoretical fundamental mode period to fit the observed Mira relation of Feast et al. (1989) (dot-dashed line)) and first (P_1), second (P_2) and third (P_3) overtone modes are shown. Colours of the points are as in figure 6.

It is interesting that, with only a few exceptions, all of the red giants with red colours ($J - K > 1.4$) reside in the brighter magnitudes of sequences *C* and C'. According to Nikolaev & Weinberg (2000), stars with $J - K > 1.4$ in the LMC are primarily carbon-rich AGB stars, being considered as the descendants of oxygen-rich AGB stars. We subdivided stars on sequences *C* and C' into two subgroups on the basis of their $J - K$ colour, being redder than 1.4 and the others. Table 3 (see section 3.3) infers that those two populations may follow the different *PK* relations, and the carbon-rich ($J - K > 1.4$) stars could define a line of somewhat shallower slope with brighter zero point than that of the oxygen-rich stars. Feast et al. (1989) obtained *PK* relations for carbon- and oxygen-rich stars in the LMC. The calculated slopes and zero-points are in good agreement with their results. In figure 8, we plotted colour-magnitude and colour-colour diagram of probable carbon-rich stars on sequence *C* and C'. Interestingly, all of the carbon-rich stars with $J - K$ colour redder than 2.0 are on the sequence *C*, meaning that all of them are pulsating in the fundamental mode. However, it should be emphasized that the obscured oxygen-rich stars such as OH/IR stars could have redder colours. So, it could be dangerous to assume that all of the stars with redder colours are carbon-rich stars. Infrared spectroscopic work would provide the definite conclusion on these issues.

The sequence *D* is thought to be populated by the longer period of a binary system (Wood 2000). However, the explanation of this sequence is not clear yet. The periods of the group *D* stars are very long and more long-term observations are needed for the clear explanation. Wood et al. (1999) suggested that stars on the loose sequence *E* are contact and semi-detached binaries. Interestingly, their distribution seems to extend to the TRGB. Stars on sequences *F* and *G* are very regularly pulsating and have periods ranging from less than 1 day to more than 30 days, suggesting that they are Cepheid variables pulsating in fundamental and first overtone mode, respectively.
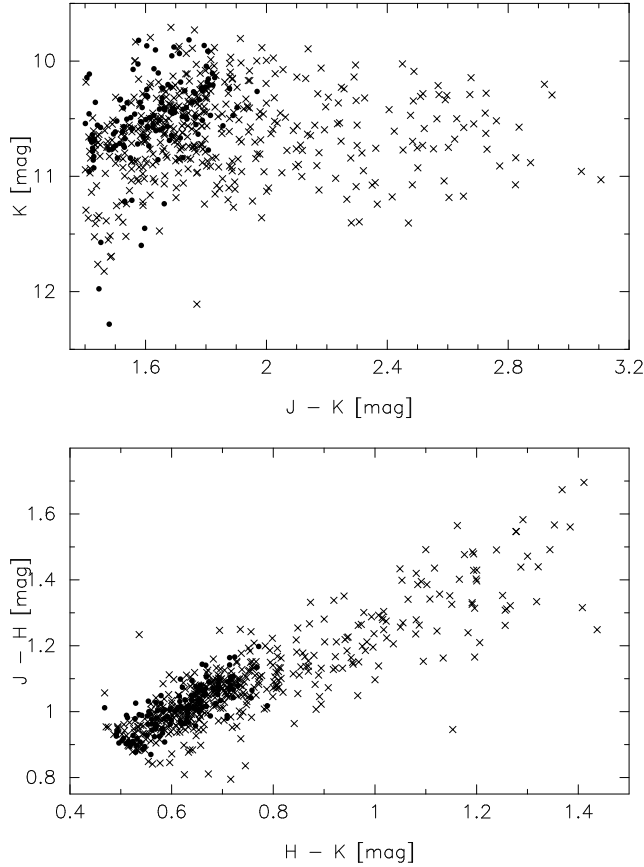
Figure 8. Colour-magnitude (upper panel) and colour-colour (lower panel) diagram of the carbon-rich stars on sequence C (crosses) and C' (dots). Two stars that are on sequence C are excluded from the colour-colour diagram, because they are outside the range.

3.3 Period-K magnitude relations

In order to determine the PK relations, we defined boundary lines as in figure 9 that divide the variable stars into nine (LMC) and eight (SMC) prominent groups (sequence E is excluded). For groups C, C' and D the slopes of the boundary lines were chosen to be -3.85, which is obtained by Hughes & Wood (1990) for the slope of the PK relation for the blend populations of carbon- and oxygen-rich Miras in the LMC. The slope of the right side of group B^+ was also chosen to be -3.85. For groups A^-B^-, A^+B^+ and FG, the slopes of the boundary lines were chosen to be -3.35, -3.45 and -3.36, respectively, after the rough estimation of the slopes of each sequence. The width of the each box was chosen so that each of them contains the most probable body of a sequence and it minimizes the miss-classifications as much as possible.

Because the scattering is rather large due probably to the SMC's intrinsic front-to-back depth, we did not tried to separate C' stars from B^+ ones in the SMC. Also, we did not calculate the PK relations of variable red giants in the SMC. The dotted lines in figure 9 are the least square fits of linear relation to each group, and table 3 summarizes the calculated PK relations.

3.3.1 Metallicity effects on the period-K magnitude relations

Gascoigne (1974) empirically obtained the period-visual magnitude relation for Cepheid variables and found that Cepheids in
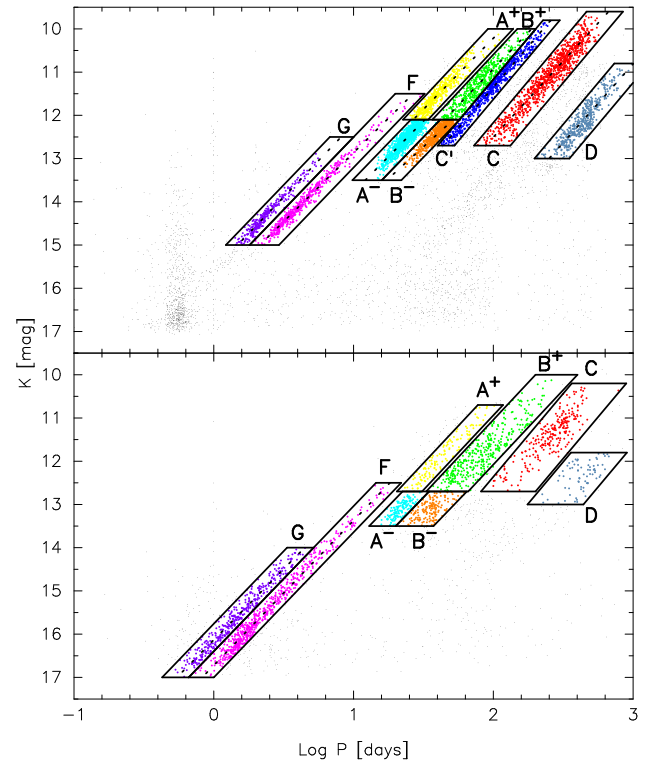

Figure 9. Period-K magnitude diagram for OGLE variables in the LMC (upper panel) and the SMC (lower panel) with classification boxes. The dotted lines are the least-square fits of linear relation to stars in each box.

the metal deficient environment would be fainter than those with the same periods in the metal rich one. Based on this result, the Cepheids in the metal-deficient SMC should be fainter than those in the LMC if compared with the same period. On the other hand, Wood (1990) suggested that if there was a factor of 2 difference in metal abundance between LMC and SMC long period variables (e.g., Miras), the LMC stars were fainter by 0.13 magnitudes in K than those in the SMC with the same period. Therefore, Cepheids and long period variables are expected to express completely different reactions to the metal abundance.

One possible way to test this anticipation is to compare the PK relations in the LMC and SMC, and it is done in figure 10. The distances to the Magellanic Clouds are still uncertain, and we can only say with confidence that the SMC lies some 0.4-0.6 mag beyond the LMC (Cole 1998). We adopted the distance moduli to the LMC and SMC as 18.40 (Nelson et al. 2000) and 18.89 (Harries, Hilditch & Howarth 2003), respectively. These distance moduli were obtained by using the eclipsing binary systems in the Magellanic Clouds, and the technique, while not entirely geometrical (reddening estimates are required), is free from the metallicity-induced zero point uncertainties. So, we shifted the K magnitudes of the SMC stars by -0.49 magnitude to account for the different distance moduli of the SMC and LMC. The red dots represent the LMC stars and the green dots correspond to the SMC stars.

The figure shows, just as expected, that Cepheids in the SMC are fainter, but red giants in the SMC are brighter than those in the LMC if compared with the same period. Also, it is likely that the slopes of the PK relations are almost the same in the two galaxies and only the zero points seem to differ. To estimate the differences quantitatively, we fixed the slopes of the PK relations of SMC Cepheids and Miras to the corresponding LMC ones, and cal-

Table 3. Period-*K* magnitude relations for variable stars in the Magellanic Clouds of the form $K = a \times \log P + b$. The *K* magnitudes are referred to the LCO system (Persson et al. 1998). The σ is the standard deviation in *K*, and *N* is the number of stars being used in the least square fitting after applying 3.0 σ clipping. Stars on sequences *C* and *C′* in the LMC were subdivided into two subgroups according to their *J − K* colour, and their period-*K* magnitude relations were also calculated.

| Group	a	b	σ	N	$J - K$
LMC					
A^-	-3.284±0.047	17.060±0.065	0.114	1142	All
A^+	-3.289±0.047	16.793±0.077	0.125	510	All
B^-	-2.931±0.057	17.125±0.091	0.100	584	All
B^+	-3.356±0.052	17.634±0.099	0.160	502	All
$C′$	-3.768±0.023	18.885±0.046	0.110	693	All
$C′$	-3.682±0.109	18.720±0.245	0.122	135	>1.4
$C′$	-3.873±0.031	19.081±0.060	0.105	558	⩽1.4
C	-3.520±0.034	19.543±0.082	0.198	975	All
C	-3.369±0.099	19.165±0.250	0.200	447	>1.4
C	-3.589±0.055	19.698±0.126	0.196	528	⩽1.4
D	-3.635±0.078	21.718±0.207	0.198	472	All
F	-3.188±0.019	16.051±0.013	0.095	540	All
G	-3.372±0.041	15.574±0.016	0.091	317	All
SMC					
F	-3.350±0.020	16.722±0.010	0.139	606	All
G	-3.280±0.035	16.133±0.009	0.147	403	All
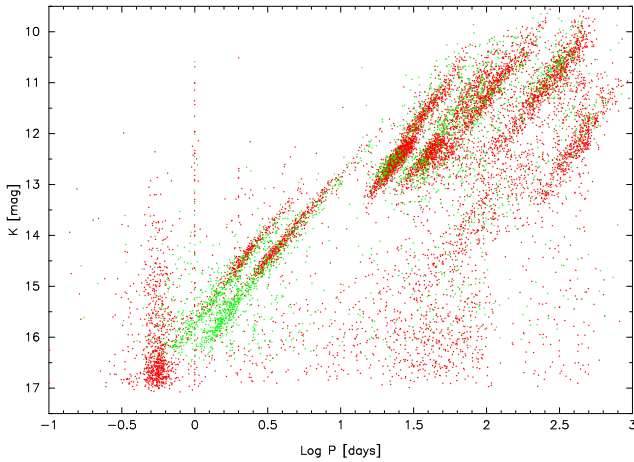
Figure 10. Period-*K* magnitude diagram of variable stars in the LMC (red dots) and SMC (green dots). The *K* magnitudes of SMC stars are shifted by −0.49 magnitude (see text) to account for the difference in the distance moduli between the LMC and the SMC.

culated the zero points. The fixed-slope solutions yielded the zero points of 19.409±0.018, 16.170±0.006 and 15.659±0.007 mag for sequences *C*, *F* and *G* in the SMC, respectively (after shifting their *K* magnitudes by −0.49 mag). Comparing these zero points with those of the LMC Cepheids and Miras, Cepheids in the SMC are fainter by ≈ 0.1 mag and Miras in the SMC are brighter by ≈ 0.13 mag than the LMC ones with the same period.

4 SUMMARY

We cross-identified the OGLE-II survey data and the SIRIUS NIR data in the Magellanic Clouds. Based on the large and homoge-

neous data[1], we studied the pulsation properties of variable stars in the Magellanic Clouds. We discovered a new sequence on the period-*K* magnitude plane, and identified it as the one for Mira variables pulsating in the first overtone mode. We also found that the variable red giants in the SMC form parallel sequences in the period-*K* magnitude plane, just like those found by Wood (2000) in the LMC. The period-*K* magnitude relations were derived, especially for both fundamental mode and overtone Cepheids in the Magellanic Clouds. These results are obtained with the greatest numbers of available stars and most deep photometric data in the infrared up to now. Metallicity effects on period-*K* magnitude relations are studied by comparing variable stars in the Magellanic Clouds. The result suggested that Cepheids in the metal-deficient SMC are fainter than the LMC Cepheids, while Miras in the SMC are brighter than the LMC ones if compared with the same period.

REFERENCES

Afonso C. et al., 1999, A&A, 344, L63
Alcock C. et al., 2000, ApJ, 541, 734
Alibert Y., Baraffe I., Hauschildt P., Allard F., 1999, A&A, 344, 551
Alvarez R., Mennessier M.-O., 1997, A&A 317, 761
Alves D. et al., 1998, in Takeuti M, Sasselov D. D., eds, Proc. IAU JD 24, Pulsating Stars: Recent Developments in Theory and Observation. Universal Academic Press, Tokyo, p. 17
Bedding T. R., Zijlstra Albert A., Jones A., Foster G., 1998, MNRAS, 301, 1073
Bessell M. S., Scholz M., Wood P. R., 1996, A&A, 307, 481
Bond I. A. et al., 2001, MNRAS, 327, 868

---

[1] Data of the variable stars will be published in the separate paper.

Castellani V., Degl'Innocenti S., Marconi M., Prada Moroni P. G., Sestito P., 2003, A&A, 404, 645

Cioni M.-R. L., Marquette J.-B., Loup C., Azzopardi M., Habing H. J., Lasserre T., Lesquoy E., 2001, A&A, 377, 945

Cole A. A., 1998, ApJ, 500, L137

Feast M. W., Glass I. S., Whitelock P. A., Catchpole R. M., 1989, 241, 375

Feast M. W., Whitelock P. A., Menzies J., 2002, MNRAS, 329, L7

Gascoigne, S. C. B., 1974, MNRAS, 166, 25

Glass I. S., Whitelock P. A., Catchpole R. M., Feast M. W., 1995, MNRAS, 273, 383

Groenewegen M. A. T., 2000, A&A, 363, 901

Haniff C. A., Scholz M., Tuthill P. G., 1995, MNRAS, 276, 640

Harries T. J., Hilditch R. W., Howarth I. D., 2003, MNRAS, 339, 157

Hughes S. M. G., Wood P. R., 1990, AJ, 99, 784

Ita Y. et al., 2002 MNRAS, 279, L32

Koornneef J., 1982, A&A, 107, 247

Lebzelter T., Schultheis M., Melchior A. L., 2002, A&A, 393, 573

Melchior A.-L., Hughes S. M. G., Guibert J., 2000, A&AS, 145, 11

Nagashima C. et al., 1999, in Nakamoto T., ed., Star formation 1999, Nobeyama Radio Observatory, p. 397

Nagayama T. et al., 2002, Proc. SPIE, 4841-51, 2002

Nelson C. A., Cook K. H., Popowski P., Alves D. R., 2000, AJ, 119, 1205

Nikolaev S., Weinberg M. D., 2000, ApJ, 542, 804

Persson S. E., Murphy D. C., Krzeminski W., Roth M., Rieke M. J., 1998, AJ, 116, 2475

Schechter P. L., Mateo M., Saha A., 1993, PASP, 105, 1342

Stellingwerf B. F., 1978, ApJ, 224, 953

STScI, 2001, VizieR Online Data Catalog, 1271

Udalski A., Kubiak M., Szymański M., 1997, AcA 47, 319

Udalski A., Szymański M., Kubiak M., Pietrzyński G., Soszyński I., Woźniak P., Żebruń K., 1999a, AcA 49, 201

Westerlund B. E., 1997, The Magellanic Clouds. Cambridge Univ. Press, Cambridge

Whitelock P. A., Feast M. W., 2000, MNRAS, 319, 759

Wood P. R., 1990, in Mennessier M. O., Omont A., ed., From Miras to Planetary Nebulae, Editions Frontières, Gif-sur-Yvette, p.67

Wood P. R., Sebo K. M., 1996, MNRAS, 282, 958

Wood P. R. et al., 1999, IAU symp., 191, 151

Wood P. R., 2000, PASA, 17, 18